Guided-Waves-Based Mortar-Filled Steel Pipe Inspection Using EMAT and Wavelet Transform

WON-BAE NA*, JEONG-TAE KIM* AND YEON-SUN RYU*

*Department of Ocean Engineering, Pukyong National University, Busan, Korea

ABSTRACT: Guided-waves-based mortar-filled steel pipe inspection is carried out through using EMAT (Electro magnetic acoustic transducer) and wavelet transform. Possibly existing anomalies such as separation (or void) and inclusion are made in the fabricated mortar-filled steel pipes; these anomalies are inspected. Since guided waves have the long range inspection capability, EMAT has its own advantages over the conventional PZT (Piezoelectric zirconate titanate), and wavelet transform gives the multi-resolution on time-frequency domain results, the suggested technique gives an alternative way for inspecting mortar-filled steel pipes, which are popularly used for supporting marine structures such as piers, wharfs, moles, and dolphins. Through this study, it is shown that the suggested technique is promising for detecting the amounts of separations and inclusions.

1. Introduction

The purpose of this study is verifying the benefits of EMATs (Electro-magnetic acoustic transducers) and CWT (Continuous wavelet transform) for guided-waves-based mortar-filled steel pipes inspection. For the purpose, experiments using EMATs are carried out and signal analysis using CWT is conducted.

Relative works can be categorized in terms of sensors used or signal analysis adopted. However, first above all, the guided-waves-based nondestructive inspections should be introduced since EMATs are used for exciting and receiving the guided waves. An excellent review by Rose (2002) introduces why guided waves are so benefiting. He introduces several advantages of the guided waves. Among them, the most benefit is the long-range inspection capability. Especially for the long pipeline inspection, the merit is invaluable. So far, many works have been done for the guided-waves-based pipe-like structures inspections. However, the mortar-filled steel pipes, which are used for supporting superstructures along with concrete-filled steel pipes, have experienced few applications of the guided waves.

In terms of sensors, PZT (Piezoelectric zirconate titanate) has been widely used and it is the most popular, stable. It is a contact sensor. Currently, non-contact sensors such as EMAT, laser, and air-coupled become popular since they have their own advantages over PZT. Thus, for nondestructive testing and evaluation, the sensor selection is wide; investigators can have more options.

In terms of signal processing or analysis, the Fourier transform experiences big challenges induced by wavelet transform. The authors believe the Fourier transform is still the master of most engineering signal processing. However, the applications of wavelet transform increases even in nondestructive testing and evaluation (Lanza di Scalea McNamara, 2004; Silva et al., 2003; Siqueira et al., 2004; Sung et al., 2002).

Through this study, it is shown that the EMATs and CWT provide excellent tools for mortar-filled steel pipe inspection when guided waves are seeking the separations or inclusions at the interface between the filling material (mortar) and the pipe (steel). Those anomalies are made for simulating the delamination at the interface between the steel pipe and the inserted mortar. Total eight specimens are tested by the experiment setup employing EMATs, and the test results are analyzed through CWT. This work suggests an alternative way for the substructure inspection, when the mortar-filled steel pipes experience the secondary defects possibly due to corrosion, which is mainly caused by sea salt and deicing materials.

2. Guided Waves

Numerous inspection techniques have been available to pipes inspection. In recent years, investigators have developed guided wave techniques for inspecting large

교신저자 나원배: 부산광역시 남구 대연3동 599-1번지
051-620-6225 wna@pknu.ac.kr

structures. These techniques have several advantages over the conventional acoustic methods: (1) guided waves can propagate a long distance; (2) there are several wave modes that can have different degrees of sensitivity to different types of defects; (3) ability to inspect structures under water, coatings, insulation, multi-layer structures or concrete with excellent sensitivity; (4) cost effectiveness because of inspection simplicity and speed; (5) they can produce surface and guide waves in any structure and material including low wave velocity composite materials. etc. (Rose, 2002). Those advantages are why many works have been done for the guided-waves-based pipe-like structures inspection in spite of the complexity of guided waves analysis, which means guided waves are dispersive and there are infinite numbers of guided wave modes (Guo and Kundu, 2000, 2001, Na and Kundu, 2002a, 2002b; Rose et al., 1994; Alleyne and Cawley, 1995; Chan and Cawley, 1995; Cheng and Cheng, 1999).

3. EMAT

Electro-magnetic acoustic transducer (EMAT) has been used as an alternative transducer for nondestructive testing. EMAT generates ultrasound waves in electric conductive materials by Lorentz force, electro magnetostrictive effect, or a combination of both. Both phenomena affect the atomic grid of the specimen so that the acoustic waves are generated directly within the specimen thus it is a non-contact device (Ogi et al., 2000). The main advantage of EMAT over conventional piezoelectric zirconate titanate (PZT) is that it does not need any couplant (Oursler and Wagner, 1995) thus we eliminate the inconsistency arising from the couplant use during the nondestructive inspection. This characteristic makes investigators attracted to EMAT for determining material properties or detecting defects in structures. Another major advantage of this device is that different guided wave modes can be generated by simply changing the coil or magnet geometry, and their sequence of excitation. Thus, the transducer can induce specific ultrasonic modes including normal beam and angle-beam shear waves, horizontal shear waves, Rayleigh waves, and Lamb waves (Maxfield et al., 1987). This helps investigators to select a transducer for a specific test. The other advantages of EMAT are: (1) it can efficiently inspect austenitic welds by using horizontally polarized shear waves (Sawaragi et al., 2000) and (2) can operate at high temperatures (Papadakis et al., 1999). However, this transducer also has disadvantages (Green, 2004): (1) EMAT can be used only for ferrous or non-ferrous metals and cannot be used for inspecting nonmetal materials such as Fiber Reinforced Polymer; (2) it

gives a relatively low transmitted ultrasonic energy and a low signal to noise ratio; (3) the induced energy is critically dependent on the probe proximity to the test object, which for practical applications is commonly maintained below 1 mm. For overcoming the major shortcomings of PZT, the requirement of a couplant, and EMAT, relatively low transmitted ultrasonic energy, a hybrid arrangement combining PZT and EMAT is used by Na and Kundu (2002c). This arrangement is used for inspecting interface defects in reinforced concrete. However, this arrangement is not necessary if the transmitted ultrasonic energy is strong enough.

In this study, EMATs for mortar-filled steel pipe inspection are used. Since the most common defect caused by the corrosion of the mortar filled steel pipe is the delamination at the interface between steel pipe and mortar, EMATs are designed for propagating guided waves through the mortar-filled steel pipe. Fig. 1 shows the layout of EMATs used for the experiment.
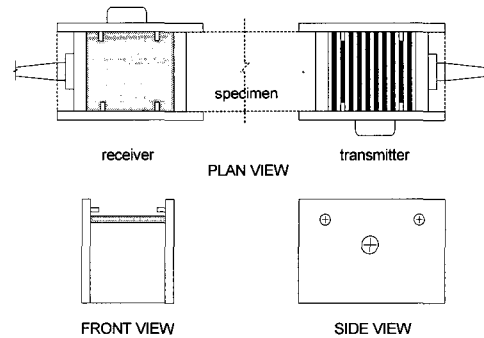

receiver PLAN VIEW transmitter

FRONT VIEW SIDE VIEW

Fig. 1 Layout of EMATs

4. Wavelet Transform

In general, raw signals are time-amplitude representations. These time-domain signals are often needed to be transformed into other domain such as frequency domain, time-frequency domain, etc. for signal analysis. Transformation of signals helps to identify distinct information, which might otherwise be hidden in the initial domain. Depending on application, the transformation techniques should be selected, and each technique has its own advantages or disadvantages.

The Fourier transform (FT) is probably the most popular transform used to obtain the frequency spectrum of a signal. However, the FT is suitable only for stationary signals, i.e. signals whose frequency content does not change with time. The FT does not tell at which time these frequency components occur, while it tells how much of each

frequency exists in the signal.

Some signals have different characteristics at different time or space, i.e. they are stationary. To analyze these signals, both frequency and time information are needed simultaneously. In other words, a time-frequency representations of the signal is required. To solve this problem, the short-time Fourier transform (STFT) was introduced. In STFT, the non-stationary signal is divided into small portions, which are assumed stationary. This is done using a window function with a chosen width, which is shifted and multiplied with the signal to obtain the small stationary signals. The Fourier transform is then applied to each of these portions to obtain the short time Fourier transform of the signal.

The problem with STFT goes back to the Heisenberg uncertainty principle, which states that it is impossible for one to obtain which frequencies exist at which time instance, but, one can obtain the frequency bands existing in a time interval (Lanza di Scalea and McNamara, 2004). This gives resolution issue where there is a trade-off between time resolution and frequency resolution. To assume stationary, the window is supposed to be narrow, which results in a poor frequency resolution. If the width of window is increased, frequency resolution improves but time resolution becomes poor. In addition, choosing a wide window may violate the condition of stationary. Consequently, depending on the application, a compromise on the window size has to be made. Once the window function is decided, the frequency and time resolutions are fixed for all frequencies and all times (Daubechies, 1992).

The wavelet transform, which was developed in the last two decades, solves the above problem to a certain extent. In contrast to STFT, which uses a single analysis window, the WT uses short windows at high frequencies and long window at low frequencies. This yields multi-resolutions at different frequencies, i.e. both frequency resolution and time resolution vary in the time-frequency plane without violating the Heisenberg inequality (Sripathi, 2003). In summary, the WT, at high frequencies, give good time resolution and poor frequency resolution, while at low frequencies, the WT gives good frequency resolution and poor time resolution.

The continuous wavelet transform (CWT) is provided by Eq. 1, where $f(t)$ is the signal to be analyzed (Mallat, 1999).

$$Wf(\tau,s) = \int_{-\infty}^{+\infty} f(t) \frac{1}{\sqrt{s}} \psi^* \left(\frac{t - \tau}{s} \right) dt \tag{1}$$

where $\psi^*(t)$ is the complex conjugate of the mother

wavelet or the basis function $\psi(t)$ defined as

$$\psi_{\tau,s}(t) = \frac{1}{\sqrt{s}} \psi \left(\frac{t - \tau}{s} \right). \tag{2}$$

All the wavelet functions used in the transformation are derived from the mother wavelet through translation (Shifting) and scaling (Dilation or Compression).

The mother wavelet used to generate all the basis functions is designed based on some desired characteristics associated with that function. The translation parameter τ relates to the location of the wavelet function as it is shifted through the signal. Thus, it corresponds to the time information in the wavelet transform. The scale parameter s is defined as $|1/frequency|$ and corresponds to frequency information. Scaling either dilates or compresses a signal. Large scales (Low frequencies) dilate the signal and provide detailed information hidden in the signal, while small scales (High frequencies) compress the signal and provide global information about the signal.

The wavelet series is obtained by discretizing CWT. This aids in computation of CWT using computers and is obtained by sampling the time-scale plane. The computation of the wavelet series may require significant amount of time and resources, depending on the resolution needed. The discrete wavelet transform (DWT), which is based on sub-band coding, is found to result in a fast computation of WT. It is easy to implement and reduces the computation time and resources required. In this study, our work is focused to CWT since the computation time is not much.

Several families of wavelets that have proven to be especially useful are introduced in the literatures (Mallat, 1999). For this study db10 (Daubechies 10) is adopted. This wavelet is orthogonal and asymmetrical (Mallat, 1999).

5. Experiment

Two sets of specimens were fabricated. The first set consists of four different mortar-filled steel pipes, containing four different degrees of separation. The second set consists of three different mortar-filled steel pipes, containing three different degrees of inclusions. In addition, one hollow steel pipe was also inspected. For the eight specimens, the average length of the pipes is 914.4mm and the outer and inner average diameters of the pipes are 22.36mm and 19.26mm, respectively. The four different degrees of separation (or inclusions) are 0%, 25%, 50%, and 75%, respectively, as shown in Fig. 2. These separations were artificially fabricated by placing wooden bars into the mortar and then extracting

those six hours after pouring mortar in the pipe. The diameter of the wooden bar is 7.90mm. Then the inclusions were made by placing wooden bars into the mortar such that the wooden bars were firmly stuck to the specimens.

An experimental setup was designed as shown in Fig. 3. The transmitter was activated by a driver and input signal was strengthened by a preamplifier. Once excited by the transmitter, the propagated cylindrical guided waves are received by the receiver. The received signal was amplified by both a preamplifier and an amplifier and then displayed on an oscilloscope as a function of time. The curves produced in this manner are denoted as time domain signals. With this setup, we do not need any transducer holder since EMAT itself has a holding mechanism.
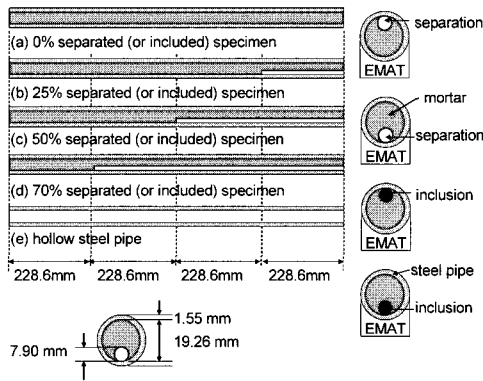
Fig. 2 Geometries of eight different specimens (left), two circumferential locations of the separation or inclusion (right)
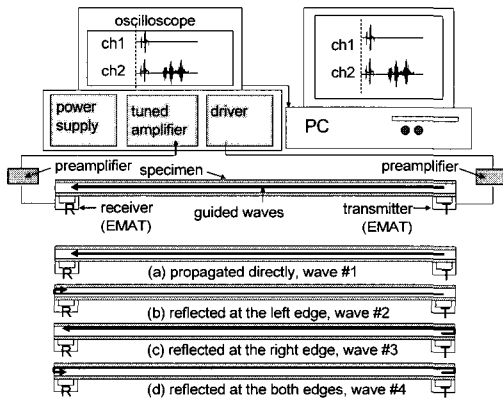

Fig. 3 The experimental setup (top), four different paths for the propagating wave (bottom)

The first step of the experiment is identifying received waves. Through the step, we figured out if the received waves are different modes or they are reflected waves from the pipe ends (see Fig. 3). The second step is to test eight

different mortar-filled steel pipes. In this step, the amount of separation (or void) and inclusion are identified. Since the void and inclusion are not axisymmetric, the circumferential location of the void may affect the experimental results. Hence, two circumferential locations of the void or inclusion are considered: (1) void or inclusion at the top segment of the pipe and (2) void or inclusion at the bottom segment of the pipe as shown in Fig. 2.

It should be noted here that the separation (or void) simulating the delamination induced by corrosion is not perfectly matched with the real phenomenon of the delamination. However, the separation (or void) itself is a very possibly existing defect when we fill mortar or concrete into the steel pipes.

6. Signal Analysis

Once the received signals arrived, we should identify the arrived wave packets. Since the guided waves can propagate different paths, the reflections can happen from the two ends of pipes as shown in Fig. 3. By measuring the group velocity of each wave packet, it was shown three wave packets in Fig. 4 and 5 give identical group velocity. It confirms that the second wave packet of Fig. 4 and 5 represents the reflected waves from the left or right edge (wave #2 and #3) and the third packet of Fig. 4 and 5 represents the reflected wave from both edges (wave #4). Thus, the three wave packets represents single wave mode. From the figures, we can also observe some wave packets in front of wave #1. These packets are supposed to be a fast wave mode and its reflected waves.

Now, we transformed the time domain signals into time-frequency domain using the Continuous wavelet transform. The mother wavelet used is db10 (Daubechies 10). Fig. 6 shows the CWT from the time-domain signals shown in Fig. 4 and Fig. 7 shows the CWT from Fig. 5. As mentioned in the previous chapter, the scale is the inverse of frequency so that at the low scales (High frequencies) in Fig. 6 and 7 we can observe the waves, which are shown in Fig. 4 and 5. Based on the Fig. 6 and 7, the CWT gives us both information of frequency and time. That is the merit of the Wavelet Transform.

The CWT is also carried out for the remained six specimens (The time domain signals are not shown here). From the Fig. 8 and 9, it is shown that the CWT is effective to quantify the separated regions. From the Fig 10 and 11, it is also shown that the CWT is effective to quantify the included regions. It seems that the results vary little depending on the circumferential location of the

separation and inclusion but overall the amount of separation and inclusion are well quantified from the CWTs. From Fig. 7, 8, 9, 10, and 11, it is shown that the values of wavelet coefficients are highest in the 0% separated (or included) specimen and the smaller separation (or inclusion) is the higher values of the coefficients are.
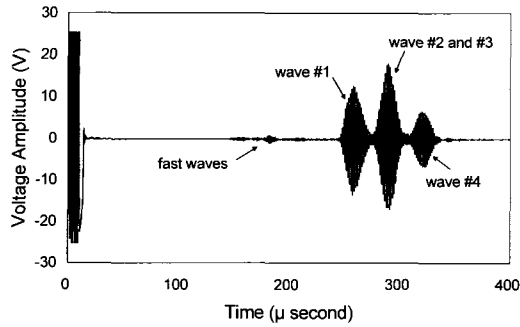

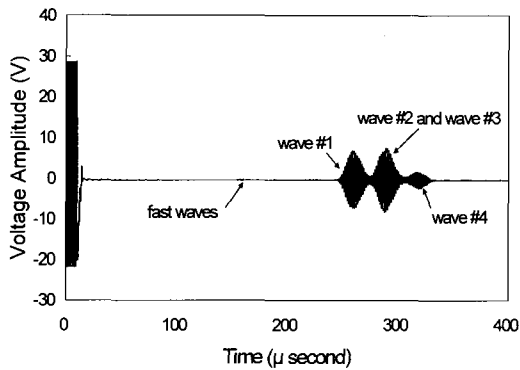**Fig. 4** Time history curves of hollow steel pipe

Fig. 5 Time history curves of 0%-separated (or included) specimen

The next question would be which wave mode is actually received. From the time domain signals in Fig. 4 and 5 it is shown that waves #1, #2, #3, and #4 are identical, which means waves #2, #3, and #4 are the reflected waves of the wave #1. Then the identification of wave #1 is the next subject we have to investigate. One of ways for the identification is investigating the group velocity dispersion curves (Na and Kundu 2002b). To calculate the dispersion curves, the material properties of the steel pipe and mortar should be known. For the steel pipe, it is relatively easy to measure the properties but not for the mortar. However, if we compare the wave packets in Fig. 4 and 5, then we can easily figure out the corresponding times to the wave peaks are identical for both the figures. For example for the peak of wave #1, the corresponding time is 258μsec for both

figures. This indicates we can use the group velocity dispersion curves of the hollow steel pipes for the mode identification. It makes our subject easy since the dispersion curves are much simpler for the hollow steel pipes than for the mortar-filled steel pipes. Hence, we obtained Fig. 12 showing the group velocity dispersions over some frequency ranges.

Now, we can plot the point obtained from the experiment, i.e. (0.694MHz, 3.193km/sec). The group velocity (3.193km/sec) is obtained by dividing the distance between the transmitter and the receiver by the time of travel (258μ sec), and the signal frequency (0.694MHz) is obtained from the record during the test. By plotting this point on the dispersion curves shown in Fig. 12, the wave mode (wave #1) can be identified. The solid square in the figure shows the point. However, L(0,1), F(1,1), and F(1,2) modes are very close at the point; hence, unfortunately we cannot decide which one is actually received. For exact identification, we need more planned experimental strategy. It should be noted here that L(0,1) is the first longitudinal axially symmetric wave mode, F(1,1) is the first flexural wave mode, and F(1,2) is the second flexural wave mode. Flexural wave modes are non-symmetric so that the fist index indicates the integer number of wavelengths around the circumference of the cylinder. The second index describes a counter variable.
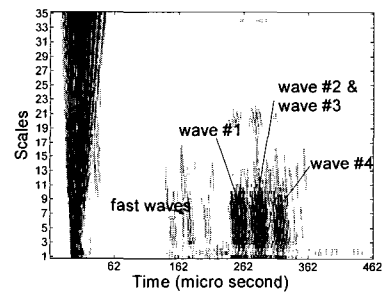

Fig. 6 Continuous wavelet transform (db 10) for the time domain signals shown in Fig. 4, the hollow steel pipe
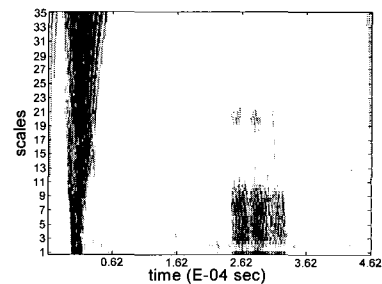

Fig. 7 Continuous wavelet transform (db 10) for the time domain signals shown in Fig. 5, 0%-separated or included
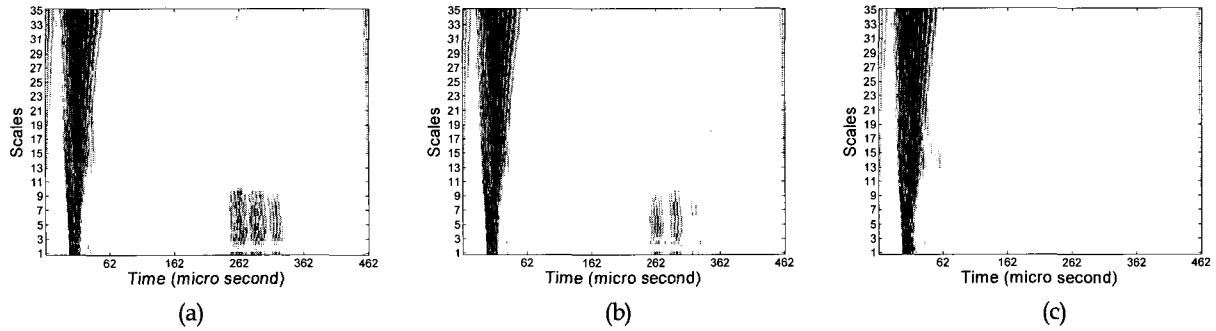
Fig. 8 Continuous wavelet transform (db 10) for (a) 25%, (b) 50% and (c) 75% separated specimens (The separations locate in the top)
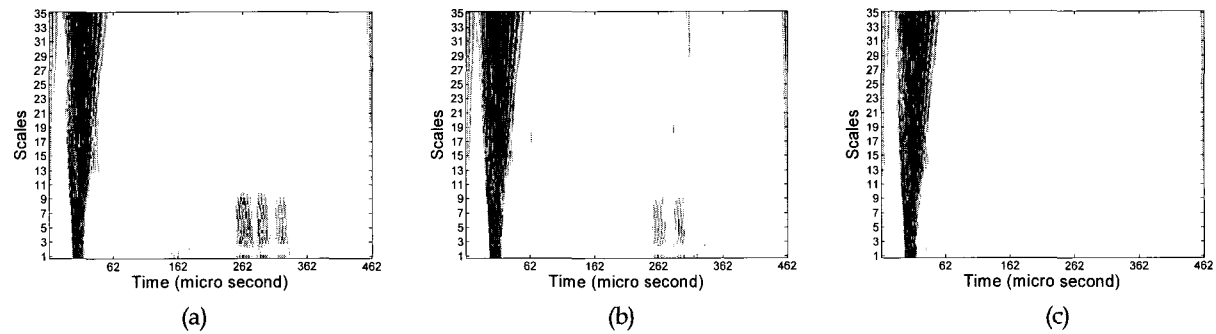

Fig. 9 Continuous wavelet transform (db 10) for (a) 25%, (b) 50% and (c) 75% separated specimens (The separations locate in the bottom)
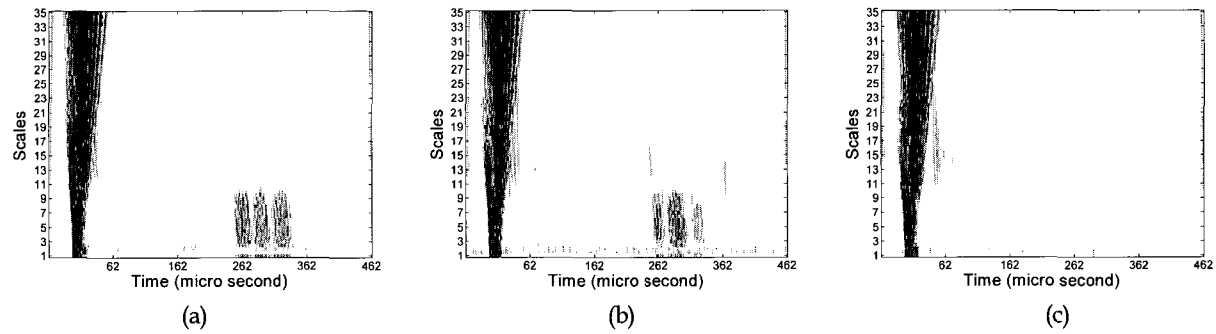

Fig. 10 Continuous wavelet transform (db 10) for (a) 25%, (b) 50% and (c) 75% included specimens (The inclusions locate in the top)
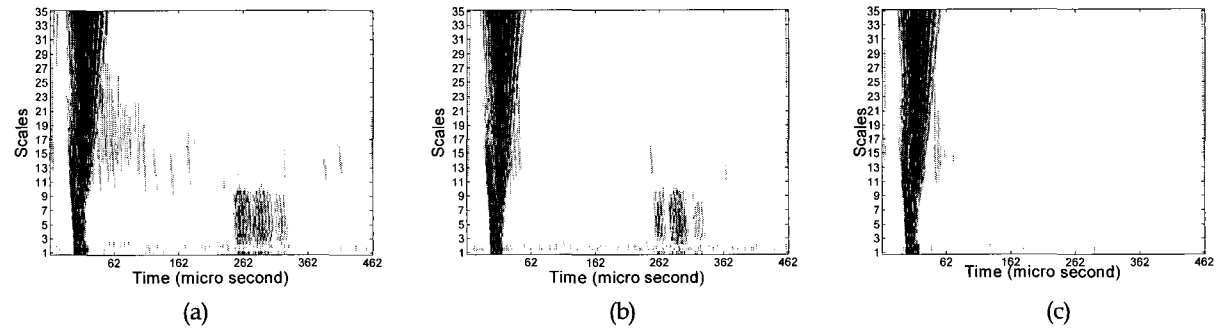

Fig. 11 Continuous wavelet transform (db 10) for (a) 25%, (b) 50% and (c) 75% included specimens (The inclusions locate in the bottom)

There would be several ways for more exact identification. One way is controlling the excited signal from EMATs such as the use of a narrow band signal (Lowe et al. 1998). This is also gives good signal strength and avoids dispersion over long propagation. Then we can plot the experiment point on the lower frequency range in the group velocity dispersion curves; hence, it may give a better chance for the identification. Another way is using a single mode generating EMAT, and then the above identification would not be necessary. However, although much work has been done in the area of development of EMAT for single mode guided wave excitation, the theoretical understanding of the physical processes involved is still very limited (Dixon and Palmer, 2004; Murayama et al., 2004; Mirkhani et al., 2004).

The other issue supposed to be discussed here is that the sensitivity of a specific guided wave mode to a certain anomaly. In this study, the anomalies are separation and inclusion. To investigate how these anomalies are sensitive to a guided wave mode, numerical and experimental works have to be carried out. Traditionally, finite element method (FEM) and boundary element method (BEM) have been used for the sensitivity analysis (Cho and Rose 2000). The simulation from FEM and BEM are very robust, producing an enormous amount of data in a single numerical experiment (Seifried et al., 2002). However, to obtain a stable solution from FEM, it is necessary to meet a number of requirements. Firstly, for numerical accuracy, the element size should at most be one eight of the shortest wavelength present. Secondly, a rapid varying mode shape over the cross-section has to be accounted for correctly by a sufficient number of elements. Thirdly, the time step for the marching procedure should not exceed 0.8 times the time in which the fastest wave can propagate on element length (Vogt, 2002). With keeping those requirements here, the sensitivity analysis remains in the future study.
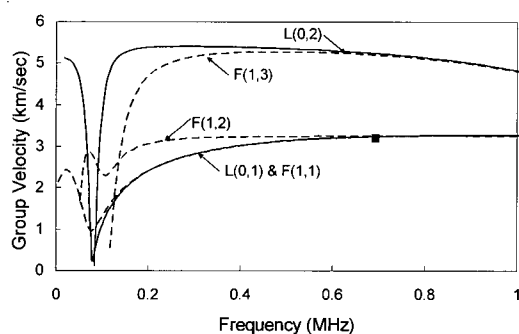

Fig. 12 Group velocity dispersion curves of the hollow steel pipe.

7. Summary and Conclusion

A guided-waves-based technique is used here for internal separations and inclusions inspection of mortar-filled steel pipes. EMATs (Electro-magnetic acoustic transducers) are used as both transmitter and receiver for generating and receiving the guided waves. From the experiment, time domain signals are experimentally obtained and then these signals are transformed to the time-frequency signals by the Continuous wavelet transform. By examining the time-frequency signals, it is shown that the amounts of separations and inclusions are well quantified. Thus, this study verifies that the guided waves techniques employing EMATs and CWT are quite effective for the separation and inclusion detections. The proposed technique can give an alternative way for maintenance and inspection of mortar-filled steel pipes, which are supporting the civil and marine structures such as bridges, piers, wharfs, moles, and dolphins. It is believed that concrete-filled steel pipes can be also inspected through the same approach.

Acknowledgement

References

Alleyne, D. and Cawley, P. (1995). "The long range detection of corrosion in pipes using lamb waves", Review of Progress in Quantitative Nondestructive Evaluation, D. O. Thompson and D. E. Chimenti eds., Vol 14B, pp 2073-2080, New York, NY, Plenum Press.

Chan, C.W. and Cawley, P. (1995). "Guided waves for the detection of defects in welds in plastic pipes", Review of Progress in Quantitative Nondestructive Evaluation, D. O. Thompson and D.E. Chimenti eds., New York, NY, Plenum Press. Vol 14B, pp 1537-1544.

Cheng, A. and Cheng, A.P. (1999). "Characterization of layered cylindrical structures using cylindrical waves," Review of Progress in Quantitative Nondestructive Evaluation, D.O. Thompson and D.E. Chimenti eds., New York, NY, Plenum Press. Vol 18A, pp 223-230.

Cho, Y. and Rose, J.L. (2000). "An Elastodynamic Hybrid Boundary Element Study for Elastic Guided Wave Interactions with a Surface Breaking Defects", International Journal of Solids and Structures, Vol 37, pp 4103-4124.

Daubechies, I. (1992). Ten Lectures on Wavelets, Society for

Industrial and Applied Mathematics.

Dixon, S. and Palmer, S.B. (2004). "Wideband Low Frequency Generation and Detection of Lamb and Rayleigh Waves using Electromagnetic Acoustic Transducers (EMATs)", Ultrasonics, Vol 42, pp 1129-1136.

Green Jr., R.E. (2004). "Non-contact Ultrasonic Techniques", Ultrasonics, Vol 42, pp 9-16.

Guo, D. and Kundu, T. (2000). "A new sensor for pipe inspection by lamb waves", Materials Evaluation, Vol 58, pp 991-994.

Guo, D. and Kundu, T. (2001). "A new transducer holder mechanism for pipe inspection", Journal of the Acoustical Society of America, Vol 110, pp 303-309.

Lanza di Scalea F. and McNamara, J. (2004). "Measuring High-Frequency Wave Propagation in Railroad Tracks by Joint Time-Frequency Analysis", Journal of Sound and Vibration, Vol 273, pp 637-651.

Lowe, M. J.S., Alleyne, D.N. and Cawley, P. (1998). "Defect Detection in Pipes using Guided Waves", Ultrasonics, Vol 36, pp 147-154.

Mallat, S. (1999). A Wavelet Tour of Signal Processing, Academic Press.

Maxfield, B., Kuramoto, A. and Hulbert, J.K. (1987). "Evaluating EMAT designs for selected applications", Materials Evaluation, Vol 45, pp 1166-1183.

Mikhani, K., Chaggares, C., Masterson, C., Jastrzebski, M., Dusatko, T., Sinclair, A., Shapoorabadi, R. J., Konrad, A. and Papini, M. (2004). "Optimal Design of EMAT Transmitters", NDT&E International, Vol 37, pp 181-193.

Murayama, R., Makiyama, S., Kodama, M. and Taniguchi, Y. (2004). "Development of an Ultrasonic Inspection Robot using an Electromagnetic Acoustic Transducer for a Lamb Wave and an SH-plate Wave", Ultrasonic, Vol 42, pp 825-829.

Na, W. B. and Kundu T. (2002a). "Underwater pipeline inspection using guided waves", Transactions ASME-Journal of Pressure Vessel Technology, Vol 124, pp 196-200.

Na, W. B. and Kundu, T. (2002b). "EMAT-Based Inspection of Concrete-Filled Steel Pipes for Internal Voids and Inclusions", Transactions of ASME-Journal of Pressure Vessel Technology, Vol 124, pp 265-272.

Na, W. B. and Kundu, T. (2002c). "A combination of PZT and EMAT for interface inspection", Journal of the Acoustical Society of America, Vol 111, pp 2128-2139.

Ogi, H., Hamaguchi, T. and Hirao, M. (2000). "In-situ monitoring of ultrasonic attenuation during rotating bending fatigue of carbon steel with electromagnetic acoustic resonance", Journal of Alloys and Compounds, Vol 310, pp 436-439.

Oursler, D.A. and Wagner, J.W. (1995). "Narrow-band hybrid pulsed laser/EMAT system for non-contact ultrasonic inspection using angled shear waves", Materials Evaluation, Vol 53, pp 593-598.

Papadakis, E.P., Oakley, C.G., Selfridge, A. and Maxfield, B. (1999). "Fabrication and characterization of transducers", Ultrasonic Instruments and Device II, Thurston, R. N. and Pierce A. D. eds., Academic Press pp 43-134.

Rose, J.L. (2002). "A Baseline and Vision of Ultrasonic Guided Wave Inspection Potential", Transactions of the ASME-Journal of Pressure Vessel Technology, Vol 124, pp 273-282.

Rose, J.L., Cho, Y. and Ditri, J.L. (1994). "Cylindrical guided wave leakage due to liquid loading", Review of Progress in Quantitative Nondestructive Evaluation, D. O. Thompson and D. E. Chimenti eds., New York, NY, Plenum Press Vol 13A, pp 259-266.

Sawaragi, K., Salzburger, H.J., Hübschen, G., Enami, K., Kirihigashi, A. and Tachibana, N. (2000). "Improvement of SH-wave EMAT phased array inspection by new eight segment probes", Nuclear Engineering and Design, Vol 198, pp 153-163.

Seifried, R., Jacobs, L. J. and Qu, J. (2002). "Propagation of Guided Waves in Adhesive Bonded Components", NDT&E International, Vol 35, pp 317-328.

Silva, M.Z., Gouyon, R. and Lepoutre, F. (2003). "Hidden corrosion detection in aircraft aluminum structures using laser ultrasonics and wavelet transform signal analysis", Ultrasonics, Vol 41, pp 301-305.

Siqueira, M.H.S., Gatts, C.E.N., da Silva, R.R. and Rebello, J. M.A. (2004). "The Use of Ultrasonic Guided Waves and Wavelet Analysis in Pipe Inspection", Ultrasonics, Vol 41, pp 785-797.

Sripahti, D. (2003). "Efficient Implementations of Discrete Wavelet Transforms using FPGAs", Master's Thesis, Florida State University.

Sung, D.U., Kim, C.G. and Hong, C.S. (2002). "Monitoring of Impact Damages in Composite Laminates using Wavelet Transform", Composites, Part B, Vol 33, pp 35-43.

Vogt, T.K. (2002). "Determination of Material Properties using Guided Waves", Doctoral Thesis, Imperial College of Science, Technology and Medicine, University of London.